npj | Materials Degradation

www.nature.com/npjmatdeg

Corrected: Author Correction

ARTICLE OPEN

Passive film characterisation of duplex stainless steel using scanning Kelvin probe force microscopy in combination with electrochemical measurements

Cem Örnek[1], Christofer Leygraf[1] and Jinshan Pan[1]

The characterisation of passive oxide films on heterogeneous microstructures is needed to assess local degradation (corrosion, cracking) in aggressive environments. The Volta potential is a surface-sensitive parameter which can be used to assess the surface nobility and hence passive films. In this work, it is shown that the Volta potential, measured on super duplex stainless steel by scanning Kelvin probe force microscopy, correlates with the electrochemical properties of the passive film, measured by electrochemical impedance spectroscopy and potentiodynamic polarisation. Natural oxidation by ageing in ambient air as well as artificial oxidation by immersion in concentrated nitric acid improved the nobility, both reflected by increased Volta potentials and electrochemical parameters. Passivation was associated with vanishing of the inherent Volta potential difference between the ferrite and austenite, thereby reducing the galvanic coupling and hence improving the corrosion resistance of the material. Hydrogen-passive film interactions, triggered by cathodic polarisation, however, largely increased the Volta potential difference between the phases, resulting in loss of electrochemical nobility, with the ferrite being more affected than the austenite. A correlative approach of using the Volta potential in conjunction with electrochemical data has been introduced to characterise the nobility of passive films in global and local scale.

npj Materials Degradation (2019)3:8 ; https://doi.org/10.1038/s41529-019-0071-8

INTRODUCTION

The nobility of metals determines their propensity to undergo reactions with a corrosive environment which is strongly related to the work function and, hence, to the Volta potential of the metal.[1,2] Less noble metals with strong passive films can outperform nobler metals with less protective surface oxides in corrosive media. For example, Fe and Cr form protective surface oxide films, and despite the lower intrinsic nobility of Cr (lower position in the EMF series) galvanic corrosion of Fe in a Cr/Fe couple occurs in many corrosive electrolytes due to the passive nature of Cr.[3] Thus, the nobility of a passivating metal (that has a strong, protective oxide/hydroxide film) is determined by the property of the passive film which has key importance in understanding corrosion.[4] The nobility of a metal in ambient air or electrolyte/corrosive environment is determined by the nobility of the metal and the oxide/hydroxide. The word 'intrinsic' implies the nobility of the metal with exclusion of the oxide/hydroxide and considers the metal's inherent, inborn, natural ability to react with or resist against the environment. This view is plausible and useful as such that, as later demonstrated, with well-thought experiments, information of the passive film (oxide/hydroxide) can be extracted and the passive film characterised to fundamentally understand mechanistic processes.

Passivity is the ability of a metal to resist against corrosion despite the thermodynamic tendency of a metal to react with a corrosive environment.[5] Passivity is furthermore the state of a metal whose corrosion rate is decreased by reaction with its environment through the formation of a surface barrier film, usually an oxide/hydroxide. The surface oxide can be further protective under anodic polarisation (noble potentials) and sustain low anodic current densities, significantly retarding metal dissolution.[5,6] Surface oxides/hydroxides usually increase the nobility and hence the resistance to corrosion.[4,6] The passive film is usually a semiconducting oxide layer having n- or p-type semiconductor properties, with n-type oxides typically being less resistive to corrosion than p-type oxides due to the Fermi level position situating closer to the conductive band.[7]

There are a variety of ways to characterise surface oxides in terms of understanding the propensity of a metal to corrosion. Electrochemical impedance spectroscopy (EIS) has often been used to gain insight into the electric characteristics of the surface oxide layer, such as resistive and capacitive behaviour.[8,9] Information about defects, anionic/cationic vacancies and the semiconductor type (n/p) can be obtained by Mott-Schottky analyses. It has, however, utmost importance to characterise the material further in local scale in order to shed light into local electrochemical processes, requiring the need for local probing techniques. It has also importance to obtain information from the outermost surface of the material since measurements of electric charges are an average of the entire volume of the surface with a certain interaction depth. So far, corrosion electrochemistry in bulk aqueous electrolytes in nanometre scale has not been achieved, and even if a clear delineation of the measured potentials or currents is needed since corrosion measurements within the

[1]Division of Surface and Corrosion Science, School of Engineering Sciences in Chemistry, Biotechnology and Health, KTH Royal Institute of Technology, Drottning Kristinas Väg 51, 100 44 Stockholm, Sweden
Correspondence: Cem Örnek (ornek@kth.se)

Received: 17 October 2018 Accepted: 1 February 2019
Published online: 19 February 2019

Published in partnership with CSCP and USTB

npj nature partner journals

electrochemical double layer (EDL), which can have thicknesses up to 100 µm, is not defined. The EDL would be perturbed by a nano-probe and possibly new EDL's would be generated, which may vary largely depending on the size, kind and geometry of the sensing probe. Therefore, measurement attempts of the corrosion potential in local scales have not only practical limitations but also theoretical concerns.

Scanning Kelvin probe force microscopy (SKPFM), instead, is one technique that can provide electronic information in nanometre scale which in turn provide insightful information into electrochemical processes, being helpful in assessing the likelihood of local corrosion events such as micro-galvanic corrosion of multi-phase alloys.[10–13] It measures the Volta potential with a sensitivity of 1 mV and a spatial resolution of ~15 nm.[12,13] The Volta potential is an intrinsic property of a metal and forms with the surface potential the Galvani potential, which describes the real electrode potential of the metal.[14–17] The Volta potential is intrinsic as such that it is always present in any condition or environment, and it is a natural, inherent occurrence or phenomenon. The Volta potential, whether measured in air or in the presence of a thin-film electrolyte, provides meaningful information about the intrinsic nobility of a metal, irrespective of the corrosive environment. Relationships between the measured Volta potential in air and the corrosion potential in chlorides have been proposed in several works, because the 'intrinsic' contribution of the metal, including the passive film to the total Volta potential in electrolyte, is often strong that it correlates with the corrosion potential. However, this cannot be generalised since the contribution of the electrolyte or the reason that the electrolyte significantly changes the surface properties can be major which can override the relationship, if any. It is useful in assessing the propensity to corrosion/oxidation in both aqueous and non-aqueous environments. There is fairly reasonable correlation between calculated Volta potentials by density functional theory and experimentally measured Volta potentials in the presence of oxides as well as adhering monolayers of water, demonstrating its usefulness in assessing the nobility of complex microstructures.[12]

In this work, SKPFM was used to assess the intrinsic (electrochemical) nobility, also known as practical or relative nobility,[10,12,18,19] of grade 2507 super duplex stainless steel (DSS) exposed to different electrochemical conditions in combination with EIS and potentiodynamic polarisation analyses performed in similar environments. Information obtained from conventional electrochemical measurements can be correlated with the Volta potential, if reported in as-measured values (e.g. no data flattening), by considering the used tip as a reference, which in turn allows the assessment of the microstructures in local scale. The main aim is to show the nobility changes in DSS microstructure associated with exposure to various environments. It will be shown that the nobility improvement of the microstructure after passivation is related to reaching Volta potential equilibrium between austenite and ferrite after which the propensity to galvanic coupling and to oxide growth significantly diminishes. It will be further shown that via SKPFM smallest changes in or on the surface can be sensed and that the Volta potential can provide meaningful information to assess the improvement and degradation of passive films of, in particular, DSS, in order to better understand localised corrosion.

RESULTS AND DISCUSSION

Nobility of phases

The ratio of the surface potential energy to the work function of a metal increases from monovalent to polyvalent metals in the sense that for the latter the surface contribution is a large part of the measured work function.[14] The Volta potential (energy), thus, is largely influenced by the contribution of the surface potential (energy), and hence adhering oxides/hydroxides[1] or water[14] (positive surface potentials) can largely increase the work function of the material, thereby improving the nobility. The work function is an energy and, therefore, in order to associate it with the surface or Volta potential, the physical involvement of charge is needed, which is done by the multiplication of potential by the energy unit of the electron or the amount of charge that has passed. Thus, we use the term surface or Volta potential energy to associate it with the work function. Figure 1 summarises the SKPFM measurement results. The average Volta potential of the entire DSS microstructure after OPS polishing was +100 mV vs. Pt, with the austenite (γ) showing 40–70 mV nobler values than the ferrite (δ) (Fig. 1, line a), indicating a different surface composition of the austenite than that of the ferrite. The bulk chemical composition of the two phases are different, and ferrite is typically rich in Cr and Mo while austenite is rich in Ni, Mn and N, resulting in usually higher corrosion potentials for the austenite than the ferrite.[20,21] Ni is known to propel Cr and Mo towards the outermost surface,[5,22,23] which may further explain the higher nobility (and also the nobler corrosion potential) of the austenite than that of the ferrite despite its lower bulk concentrations of Cr and Mo (Fig. 1).

Effect of nitric acid oxidation on the nobility

Immersion in concentrated nitric acid (classic passivation treatment) led to an ennoblement of the entire microstructure, which became apparent from the increased Volta potentials (Fig. 1, line b). The Volta potential difference between ferrite and austenite, however, vanished, and both phases were seen to lose nobility with time (Fig. 1, lines b–d), apparent from the decreasing Volta potentials with time (note the measurement direction). Seemingly, the average Volta potential of the entire microstructure reached (near) steady-state conditions (line d in Fig. 1), and it was similar to the average Volta potential at the beginning (line a in Fig. 1). This suggests that the passive films of both ferrite and austenite were of different character but became similar or identical due to nitric acid treatment as the Volta potential contrast vanished and both phases assumed similar values. Hence, the nobility of the microstructure improved as the Volta potential difference between the phases vanished, indicating no galvanic coupling.

Effect of nitric acid oxidation on the passive film

Nitric acid is a strong oxidant, and stainless steels spontaneously passivate in concentrated nitric acid solutions and remain passive at open-circuit potential (OCP) conditions.[24] Laurent et al. investigated two stainless steels with low and high Si content in nitric acid and concluded that their passive layer was similar at the end of passivation. The naturally formed passive film over the ferrite is different than that of the austenite, giving rise to a typical Volta potential difference of 40–70 mV of numerous DSS's.[12,13,19,25] Laurent et al.[24] reported a chromium-rich oxide, in the form of chromia, that became further enriched in the passive film upon passivation in nitric acid, with the thickness, however, not been majorly altered. This may explain the reason why the Volta potential of ferrite and austenite of the DSS were similar after immersion in nitric acid. The chromia in the passive film of the investigated DSS has been earlier demonstrated to be nanocrystalline and to be composed of a metal oxide/hydroxide mixture, consisting mainly of Fe and Cr but also some Mo and Mn species.[6]

Chromia has a p-type semiconductor property, and a high work function of ≈5 eV was reported for Cr_2O_3(0001).[26] The passive film of stainless steels is known to be composed of an outer iron-rich oxide, mainly Fe_2O_3 and $Fe(OH)_2/Fe(OH)_3$, and an inner chromium-rich oxide, often stated as Cr_2O_3 and $Cr(OH)_3$, with also some molybdenum as well as silicon species.[22–24,27] The composition and morphology as well as defect contents and semiconductor properties of passive films of stainless steel can largely differ

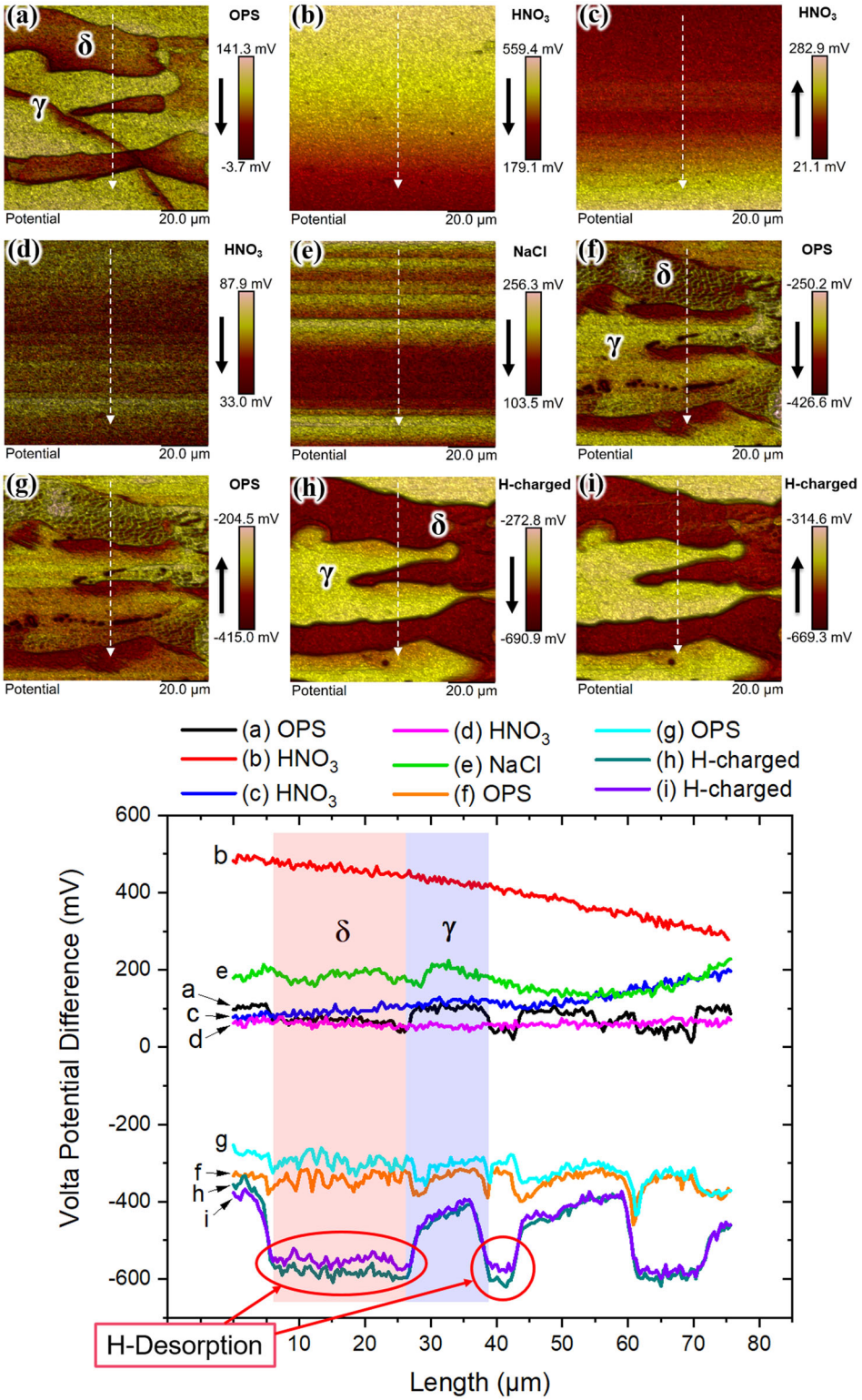

Fig. 1 Volta potential development as a function of different surface conditions. The dashed lines in the potential maps show the position of local Volta potential extractions shown in the graph. The black arrows next to the maps show the scan direction

depending on the environment in which they form. In earlier work, it was shown that the native passive film on the studied alloy gets more defective upon anodic polarisation from its passive to transpassive potential regime in 1 M NaCl solution, and becomes thicker and changes its composition and structure.[6] Marcus et al. reported passive films of stainless steels to be amorphous at the onset of oxidation and becoming crystalline by time.[23,28,29] It is therefore likely that the passive film after immersion in nitric acid became amorphous but had the tendency to transform to a crystalline structure as indicated by the change of the Volta potential by time. The passive film after the nitric acid treatment was imperfect, and some reconstruction processes

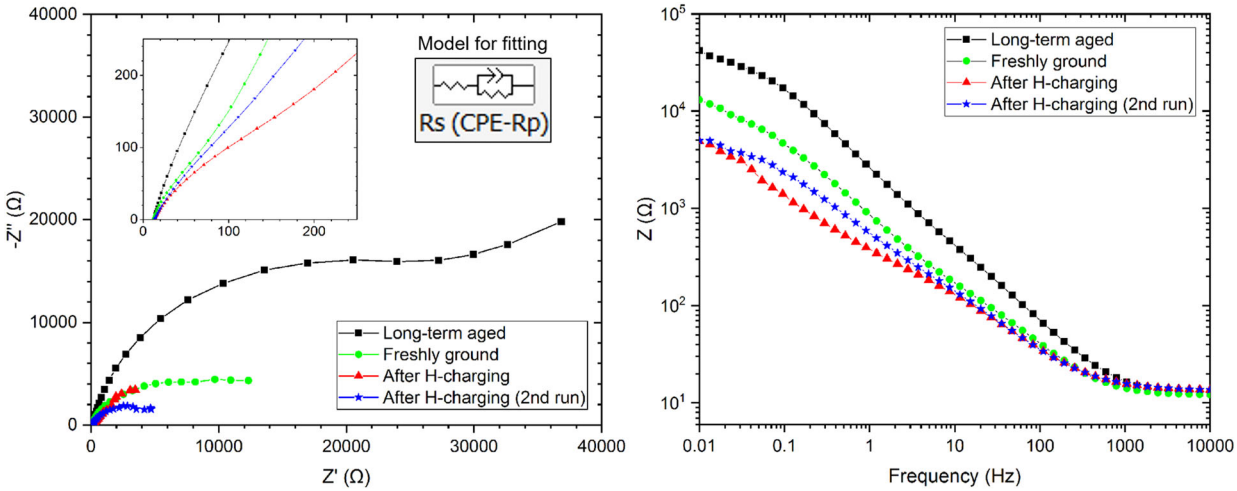

Fig. 2 EIS spectra collected in 1 M NaCl solution at room temperature. Nyqvist (left) and Bode (right) plots. The equivalent electrical circuit used for fitting of the EIS data is shown in the Nyqvist plot

governed the Volta potential changes. The treatment, clearly, led to an electronic modification of the surface layer since charging lines in the Volta potential maps (spontaneous rises and drops) were seen (Fig. 1, line d). The measurements demonstrate the uniqueness of the sensitivity of SKPFM, which can follow structural and compositional changes of the surface oxide of metals.

Effect of chloride on the nobility/passive film

Short immersion (seconds) in 1 mM NaCl solution revealed to some extent the phase contrast but the charging lines remained (line e in Fig. 1). The interaction of chloride ions with surface oxides can be manifold, and ion migration/penetration into the oxide and adsorption/ion displacement, leading to oxide thinning, have often been reported.[30] The oxide film's electrical resistance of stainless steels as well as aluminium was shown to increase with incorporated chloride into the passive film,[30,31] which may explain the reason for the increasing Volta potentials (nobler values) upon the short immersion in 1 mM NaCl. The short immersion has apparently not led to local breakdown of the passive film as an increase of the Volta potential was observed. Sato[7] introduced an electro-capillary breakdown model of passive films by chloride ions and argued that no breakdown can occur when the dissolution power of the electrolyte is low, i.e. when the steel is polarised not higher than its repassivation potential. Grade 2507 DSS is a very high corrosion-resistant material, in particular at room temperature where pitting is not possible, and it is not surprising that adhering chloride after immersion in 1 mM NaCl increased the Volta potential of the surface (SEM-EDX analysis after immersion of the DSS in chloride solution revealed eminent chlorine signal). It will be shown later that the steel is continuously passivating in 1 M NaCl solution, which results in improved polarisation resistance and corrosion properties.

Chemico-mechanical polishing with OPS for 10 min re-revealed the potential difference between ferrite and austenite (Fig. 1, line e). However, the average Volta potential dropped by ≈450 mV, with the ferrite having slightly lower nobility than the austenite. The microstructure after chemico-mechanical polishing is typically not flat, and the austenite usually protrudes the surface. Therefore, the recessed ferrite and the interphase boundary regions were less polished and thus less affected. The OPS polishing treatment removed the adsorbed nitrates/chlorides from the surface as well as the oxides, but seemingly not entirely. The Volta potentials 10 min after the previous scan (Fig. 1, lines f, g) increased by ≈20–50 mV, indicating oxidation and/or restructuring of the surface (relaxation and/or reconstruction), leading to an ennobled surface (Fig. 1, line g).

Effect of hydrogen on the nobility/passive film

Cathodic potentiostatic polarisation in 0.1 M NaOH solution at −700 mV vs. Ag/AgCl (sat.) for 10 min decreased the Volta potentials and increased the potential contrast between ferrite and austenite up to 200 mV (Fig. 1, line h). The austenite became the nobler phase again and the microstructure showed stronger galvanic coupling due to larger Volta potential differences (130–200 mV). Passive film thinning with also possible removal can occur during cathodic polarisation.[32] The cathodic reaction (during cathodic polarisation) at and above near-neutral pH is the reduction of water to atomic hydrogen and hydroxyl ions:[33]

$$H_2O + e^- = H + OH^-. \quad (1)$$

Hydrogen can migrate rapidly into metals, and the ferrite can absorb more hydrogen per time than austenite due to higher diffusivities,[34,35] causing strain localisation in the DSS microstructure.[25] The solubility of hydrogen, however, is typically two orders of magnitude higher in the austenite than in the ferrite due to its closed-packed structure, but the austenite can accommodate more lattice strain due to its face-centre-cubic structure.[36,37] Hydrogen diffusion into austenite is retarded and requires more energy, but once hydrogen has infused the effusion rate will be significantly slower than that of the ferrite.[34,35] Hydrogen can affect the passive film and also create defects, and possibly also perturbs the crystalline nature of the oxide.[38–40] In this work, hydrogen was seen to reduce the nobility of the entire microstructure, with the ferrite being more affected than the austenite. A strong galvanic coupling would be expected between both phases, and it has been reported that the corrosion resistance of DSS's was reduced after hydrogen charging, with corrosion pits preferentially nucleated in the austenite as well as interphase boundaries.[39,40] The same measured area after ≈10 min showed increasing Volta potentials of the ferrite by 20–40 mV, whereas no significant changes were measured on the austenite (Fig. 1, line i). Hydrogen diffusion and effusion/desorption is 4–5 orders of magnitude faster in ferrite than in austenite, which explains this observation.

Electrochemical evidence for the nobility changes

Figure 2 shows EIS spectra obtained in 1 M NaCl solution for different surface conditions. The reason for using 1 M NaCl was to demonstrate the superior resistance of the super duplex steel to

Table 1. Extracted electrochemical data from fitting of the EIS data shown in Fig. 2

Test no.	Condition	Rs [Ω cm²]	CPE-T [F cm²]	CPE-P	Rp [Ω cm²]
1	Long-term aged[a]	11.6 ± 0.3	$7.8 \times 10^{-5} \pm 10^{-6}$	0.82 ± 10^{-4}	46,400 ± 3000
2	Freshly polished[a]	11.2 ± 0.4	$2.8 \times 10^{-4} \pm 10^{-5}$	0.73 ± 10^{-4}	14,200 ± 1700
3	H-charged[b]	—	—	—	—
4	H-charged[a]	12.3 ± 0.3	$4.8 \times 10^{-4} \pm 10^{-5}$	0.67 ± 10^{-3}	6700 ± 450

No. 3 was measured 60 s after hydrogen charging (≈16 min measurement time)
No. 4 was measured 60 s after previous step (≈16 min measurement time)
[a]Analysed with the equivalent electrical circuit shown in Fig. 2
[b]Data fitting was not possible using equivalent electrical circuit shown in Fig. 2

chloride corrosion in ambient environment. SKPFM after immersion in 1 M NaCl revealed too much charging, which indicated no/low surface conductivity. The impedance modulus values (low-frequency limit gives the polarisation resistance, R_p) at low frequencies were highest after long-term ageing (naturally oxidised) as contrasted to the freshly ground condition (4000-grit finish). The polarisation resistance was further reduced upon cathodic hydrogen charging, indicating loss of electrochemical nobility. The polarisation resistance markedly reduced after hydrogen charging (Fig. 2), in line with the SKPFM measurements. Most of the EIS spectra essentially exhibit a time constant feature, so the equivalent electrical circuit shown in Fig. 2 (left) was used for data fitting, except the spectrum obtained immediately after the hydrogen charging. A constant phase element (CPE) was used to account for non-homogeneity in the electrochemical system. Stainless steels are passive per se and therefore the electrical circuit shown in Fig. 2 (left) is plausible. The fitting results are summarised in Table 1. The lowest *T*-value and a highest *P*-value (also known as *n*-value) of the CPE were obtained for the long-term aged condition among all other conditions, indicating the capacitive behaviour of the aged oxide in the passive film, giving a high R_p. In contrast, the *T*-value was increased while the *P*-value decreased after hydrogen charging indicating degradation of the passive film, being in line with the reduction of R_p. Immediately after the hydrogen charging, the surface must have been highly altered due to hydrogen charging since the spectrum exhibited two-time constant features, so data fitting was not possible using the circuit shown in Fig. 2 (left). In this case, it is reasonable to consider a diffusion process (effusion of hydrogen) in the interpretation of the spectrum. A diffusional feature (e.g., Warburg element) appears typically in the spectrum when a reactant or product involving in the interfacial charge transfer reaction diffuses through the electrolyte or the electrode material. The impedance at low frequencies may correspond to diffusion deeper into the material. In addition to the diffusion in the electrolyte, the thin surface oxide layer (~2 nm) creates a finitely-long diffusion layer for ionic transport through the solid material leading to diffusional impedance corresponding to diffusion of a reacting species to or from the electrode/electrolyte interface.

Upon termination of cathodic charging, most of the hydrogen usually effuses from the surface, which can recombine at the surface and/or oxidise to H_3O^+ ions, giving rise of the diffusional impedance in the spectrum. The hydrogen in the ferrite effuses faster than that in the austenite. Immediately after H-charging, there will be a large concentration of atomic hydrogen streaming out from the surface, which apparently led to a nobility loss of the passive film (Volta potential drop), and was also reflected by the impedance spectra. The EIS spectra clearly showed that the large changes in both Nyqvist and Bode plots (Fig. 2) were associated with the hydrogen charging. A repeated measurement (second run) after ca. 16 min was carried out, and the pH near the sample surface was measured during and after galvanostatic charging in order to confirm hydrogen effusion had occurred. The initial pH of the solution was 6.4 ± 0.1, which increased during hydrogen charging and reached 6.8 ± 0.1 at the end of cathodic polarisation (10 min at 10 mA/cm^2, corresponding to a potential of −1.54 $V_{Ag/AgCl}$). After termination of cathodic polarisation, the pH continuously decreased to 5.12 ± 0.01 within 10 min. This clearly showed that a significant fraction of hydrogen during effusion was anodised to H^+, which resulted in a decrease of the pH. During cathodic hydrogen charging, the pH increased to higher values due to the hydroxide ions produced (see Eq. 1), which apparently was the rate-determining step. Proton transport (hopping) is typically ultrafast and diffusion rates of 9×10^{-1} m^2/s have been reported in aqueous solution.[41] In contrast, the hydrogen diffusion rate is in the order of 10^{-11} m^2/s for the ferrite and 10^{-16} m^2/s for the austenite.[42] Thus, after termination of the hydrogen charging, the hydrogen effusion rate was 10–15 orders of magnitude slower than the H^+ transport in the electrolyte. Therefore, the hydrogen effusion from the surface was the rate-determining step of the coupled anodic and cathodic reactions at the OCP, explaining the diffusional response in the impedance spectrum. Hydrogen effusion occurred faster on the ferrite than the austenite, in line with the SKPFM measurements that clearly showed more Volta potential changes occurring over the ferrite than the austenite (Fig. 1). The surface after hydrogen charging suffered significantly from nobility loss, as manifested by a drop in the polarisation resistance (impedance modulus at low frequencies seen in Bode plot in Fig. 2) as well as a drop in the Volta potential (more anodic values seen in Fig. 1).

Passive film properties vs. nobility

The polarisation resistance of the DSS was highest for the long-term aged condition (Table 1), which demonstrates that the quality of the passive film of the DSS improves by natural ageing. The polarisation resistance was significantly lower when the surface was in its freshly polished condition, and it was further decreased when hydrogen is present in the surface/microstructure (Table 1). Hydrogen apparently affected the quality of the passive film, resulting in high conductivity (reduced resistive ability) of the passive film, in line with other works.[38,43] Moreover, the OCP data and polarisation curves in Fig. 3 demonstrated that the freshly ground DSS was passivating in 1 M NaCl solution. Lower anodic current density was seen in the passive potential region when the material was kept longer in the electrolyte prior to polarisation. No local breakdown occurred before reaching transpassivity (~1.1 $V_{Ag/AgCl}$). The polarisation curves are in agreement with the Volta potential evolution shown in Fig. 1, showing an increase in nobility with aging in air and immersion in the NaCl solution. It is generally accepted that for stainless steels, during immersion in low pH and neutral electrolyte, preferential dissolution of Fe leads to enrichment of Cr in the passive film, and hence an increased polarisation resistance.

When the surface was treated with nitric acid, however, decreasing polarisation resistance as well passive film quality

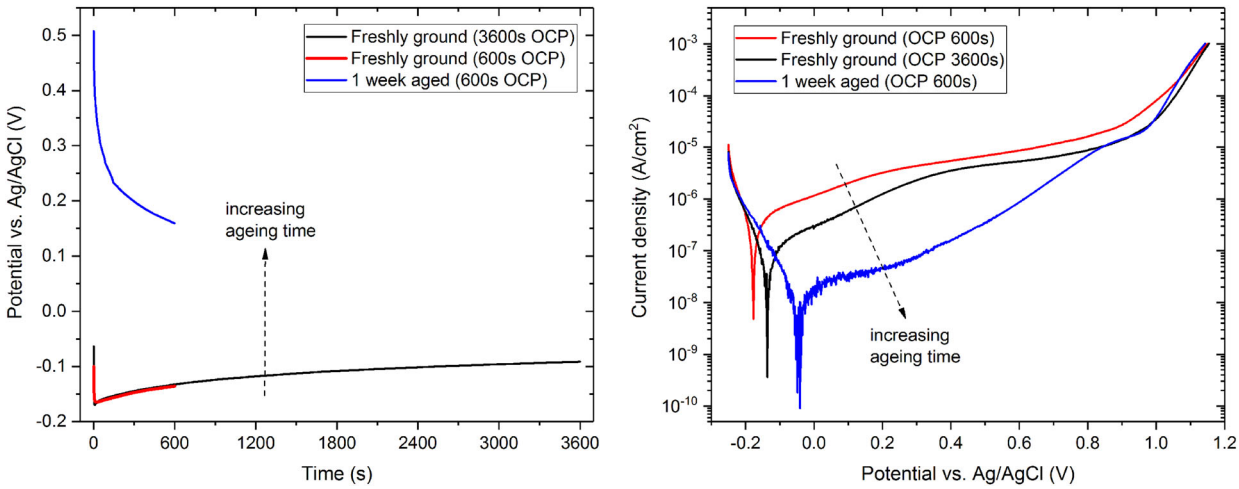

Fig. 3 OCP (left) and polarisation (right) measurement results in 1 M NaCl at room temperature. The samples were freshly ground (1200-grit SiC sandpaper) or stored in ambient air for 1 week for ageing of the passive film. The OCP measurements of freshly ground specimens were carried out for 600 and 3600 s, respectively, and the specimen aged for 1 week was tested for 600 s only. The potentiodynamic polarisation scans were conducted straight after the OCP measurements

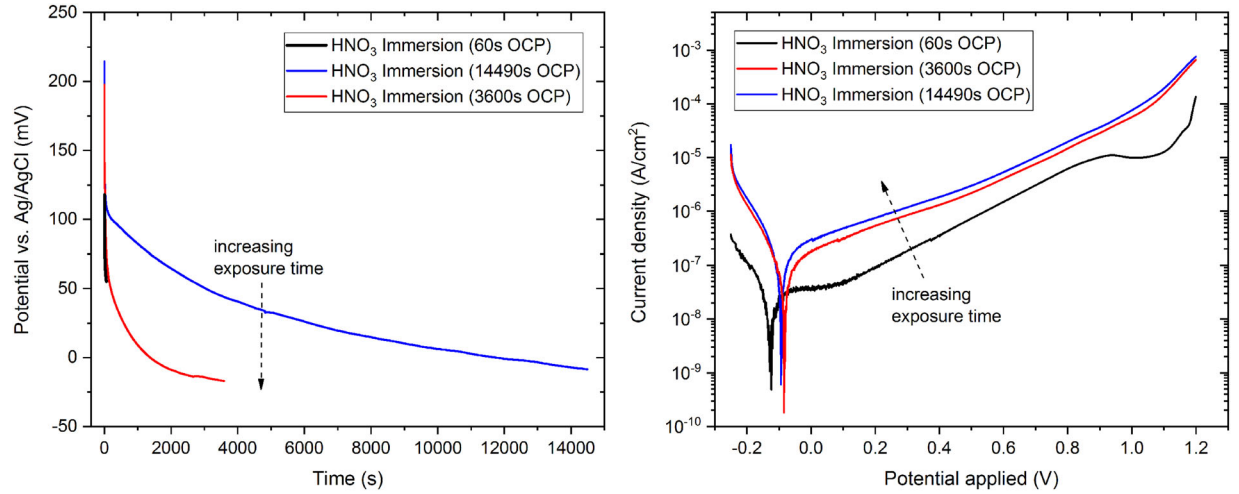

Fig. 4 OCP (left) and polarisation (right) measurement results in 1 M NaCl at room temperature. The samples were pre-immersed in concentrated nitric acid for 3 min. The OCP measurements of specimens immersed in concentrated nitric acid were carried out for 60, 3600 and 14490 s, respectively. The potentiodynamic polarisation scans were conducted straight after the OCP measurements

was seen to occur when exposed to 1 M NaCl solution prior to polarisation (Fig. 4). The OCP was seen to continuously drop and seemingly not reaching steady-state conditions after ~15,000 s (250 min). The drop of nobility (passive film quality) was also reflected by the potentiodynamic polarisation curves, which also showed increasing anodic current density (Fig. 4). This trend is in agreement with the measured Volta potentials that decreased with time indicating loss of nobility. The passive film, which was modified by concentrated nitric acid, had apparently different behaviour in the chloride-containing electrolyte as contrasted to the naturally formed passive film.

The Volta potential has been demonstrated to be a useful quantity to assess the surface nobility for characterisation of the passive oxide films of DSS. Correlation was seen between the Volta potential and electrochemical properties, both varying with exposure to various environments. It has been shown that, when such a relationship is established, SKPFM can be used to assess local nobilities to better understand localised corrosion and/or local degradation processes such as hydrogen absorption. However, extra precaution is required for the handling of the Volta potential which requires thorough understanding of the instrument, the physical meaning of the Volta potential as well as profound knowledge of both the material and the electrochemical behaviour in the studied system. The concerns raised by Rohwerder and Turcu[44] are advised to be considered when conducting such experiments. When conducting long-term SKPFM measurements a good calibration routine needs to be devised to ensure reliability of the measured data. Such concern may not be a problem for experiments that are performed in the same day (with hours) as demonstrated in this work.

The work has shown that the Volta potential is a useful parameter to characterise the surface nobility of a metal and hence the passive film, as SKPFM is sensitive to the outermost surface and provides insightful information to assess the electrochemical nobility in local scale. The approach shown in this work, hence, has shown that the native passive film over austenite is superior to that of the ferrite, reflected by higher Volta potentials, and that hydrogen infusion in DSS microstructure

causes more degradation of the ferrite than the austenite. It was further shown that the Volta potential difference between ferrite and austenite vanished upon immersion in concentrated nitric acid, indicating the adoption of similar passive film properties, thus improving the corrosion resistance of the material (no galvanic coupling). It was furthermore shown that adsorbed chloride/nitrate can improve the quality of the passive film for short-term exposures, more for the austenite than the ferrite. These observations clearly demonstrated that the Volta potential of the passive films over DSS shows correlation with the resistive and capacitive properties obtained by EIS and potentiodynamic polarisation. Thus, the Volta potential, measured by SKPFM, can be used to assess the surface nobility of metals and characterise (passive) oxide films.

METHODS

Material

The DSS investigated was SAF 2507 (UNS S32750), provided by Sandvik Materials Technology, which contained (wt%) 24.9% Cr, 6.9% Ni, 3.89% Mo, 0.77% Mn, 0.6% Si, 0.26% Cu, 0.27% N and other elements (Fe balanced). The material was solution-annealed by the manufacturer. Coupon specimens in sizes of 25 mm × 25 mm × 4 mm were cut from a plate material.

SKPFM measurements

SKPFM was used to determine the local (practical or relative) nobility of DSS microstructure in similar exposure conditions used for characterising the passive film formed in ambient air and exposed to passivating and corrosive environments. Samples were ground and polished down to 1/4 µm using diamond suspension. The measurements were done after an additional end-polishing treatment in a consecutive order beginning with (I) a modified OPS (oxide polishing suspension) solution which oxidises the surface (pH 1–2), then (II) after immersion in concentrated nitric acid, then (III) immersion in chloride-containing electrolyte (1 mM NaCl) for some seconds, and then (IV) after cathodic galvanostatic polarisation in 1 M NaCl solution using 10 mA/cm^2 at room temperature to generate hydrogen at the surface. The latter was done to see the effect of hydrogen charging on the Volta potential evolution (hydrogen-passive film interactions). SKPFM measurements were performed using an OSCM-Pt R3 n-Si doped Pt-coated tip, with 6000 mV bias voltage applied to the sample and a pixel resolution of 256 × 256. The measurements were carried out in ambient air at 21 °C and ~35% relative humidity. The frequency modulation (FM-KPFM) technique was used to measure the topography and Volta potential at the same time in single pass mode, taking 10 min to obtain one map. The Volta potential maps were not inverted (since bias was applied to the sample) and no filtering, such as smoothing, was applied to the measured data. The algebraic signs as well as the scale of the data are conformed to the electrochemical nobility convention, showing high values as noble and low values as less noble/ignoble. It should be noted that Pt is one of the most reliable reference electrodes.[17] Pt can be oxidised, but this only occurs under large anodic polarisation. The Pt-tip may have an adhering monolayer of water or may have even been oxidised during manufacturing or the long-term storage in the lab, but this does not affect the measurements since the nobility stability of Pt in ambient air was checked against a calibration reference sample (Au/Al and HOPG), which showed fairly identical values (Volta potential differences) during the same measurement day with no significant variation occurred (max. deviation was 2–3 mV). Therefore, measurements performed in ambient air, in particular for those carried out on the same day (within hours), can be regarded as relatively stable, if it can be guaranteed that the Volta potential of the tip was not affected. The latter can be verified by measurements against a reference sample (pure Au and Al) before and after the measurements, which is possible if no temperature and humidity changes occur in short time scales (maximum a few hours).

EIS measurements

EIS was used to obtain electrochemical characteristics of the passive film formed on DSS in air to see the effect of long- and short-term ageing on the corrosion resistance in aqueous chloride-containing environment (1 M NaCl) at room temperature. EIS was further employed to monitor passive film evolution upon cathodic hydrogen charging in the same electrolyte to obtain understanding about the effect of hydrogen on the surface oxide film. The measurements were aimed to correlate Volta potentials with electrochemical data (general trend) and to assess the nobility of the passive film. Samples were ground down to 4000-grit surface finish using SiC sandpapers. A specimen was exposed to ambient-air environment for ≈12 months to allow natural oxidation with the aim to obtain an aged native passive surface oxide film. Another specimen was tested in its freshly ground surface condition (4000-grit) to see the effect of ageing on the quality of the passive film. Impedance spectra were collected within the frequency range 10 kHz and 0.01 Hz (51 measurement points) using a perturbation amplitude of 10 mV. Nyquist and Bode plots were generated from the collected data. A MetroOhm potentiostat and a three-electrode electrochemical cell with a saturated Ag/AgCl reference electrode and a Pt counter electrode were used for the measurements. The sample was kept for 5 min in the solution, and the OCP was measured for 1 min prior to EIS measurements. ZView V3.5d programme was used for analysis of collected EIS data.

OCP and potentiodynamic polarisation tests

OCP and potentiodynamic polarisation measurements in 1 M NaCl solution were carried out on samples which were (I) freshly ground (1200-grit SiC sandpaper), (II) aged in air for 1 week and (III) pre-immersed in concentrated nitric acid to characterise the response of the passive film to exposure time in chloride solution and to obtain electrochemical information to better understand the effect of oxidation/passivation of the DSS. The OCP was recorded for intervals between 60 and 14,490 s followed by potentiodynamic polarisation from −250 to 1200 mV vs. Ag/AgCl with a sweep rate of 1 mV/s. The measurements were repeated to a minimum of three times, and good reproducibility was achieved (max. scatters were <100 mV and half magnitude of current density).

DATA AVAILABILITY

The datasets generated and/or analysed during the current study are available from the corresponding authors on reasonable request.

ACKNOWLEDGEMENTS

The authors are grateful for the financial supports of the Swedish Research Council (Vetenskapsrådet) through the project grant no. 2015-04490 and the Sweden-Germany collaboration grant no. 2015-06092. Sandvik Materials AB is highly acknowledged for the provision of the investigated material and also for the partial financial support for this study. Dr. U. Kivisäkk and Dr. E. Bettini at Sandvik Materials AB are also thanked for valuable discussions. The authors are grateful to Prof. P.M. Claesson at KTH Royal Institute of Technology for the fruitful discussions. This work has been funded by the Swedish Research Council (Vetenskapsrådet) through the project grant no. 2015-04490 and the Sweden-Germany collaboration grant no. 2015-06092.

AUTHOR CONTRIBUTIONS

C.Ö. devised, planned, and conducted all experiments, analysed all data, and wrote the paper. C.L. analysed the data and made inputs to the paper. J.P. analysed the data and made inputs to the paper.

ADDITIONAL INFORMATION

Competing interests: The authors declare no competing interests.

Publisher's note: Springer Nature remains neutral with regard to jurisdictional claims in published maps and institutional affiliations.

REFERENCES

1. Burshtein, R. C. The investigation of corrosion of metals and semiconductors by volta potential measurements. *Electrochim. Acta* **7**, 551–558 (1962).
2. Li, W., Cai, M., Wang, Y. & Yu, S. Influences of tensile strain and strain rate on the electron work function of metals and alloys. *Scr. Mater.* **54**, 921–924 (2006).
3. Heine, B. Untersuchungen an Eisen und Chrom sowie deren Legierungen zur Bildung und Zusammensetzung der Passivschichten auf diesen Werkstoffen (Max-Planck-Institut für Metallforschung, Institut für Werkstoffwissenschaften, University of Stuttgart, Stuttgart, 1988).
4. Schmuki, P. & Böhni, H. Metastable pitting and semiconductive properties of passive films. *J. Electrochem. Soc.* **139**, 1908–1913 (1992).

5. Marcus, P. & Maurice, V. in *Passivity of Metals and Semiconductors* (eds Ives, M.B., Luo, J.L. & Rodda, J.R.) 30–64 (The Electrochemical Society, Jasper Park Lodge, Canada, 1999).
6. Örnek, C. et al. In-situ synchrotron GIXRD study of passive film evolution on duplex stainless steel in corrosive environment. *Corros. Sci.* **141**, 18–21 (2018).
7. Sato, N. Anodic breakdown of passive films on metals. *J. Electrochem. Soc.* **129**, 255–260 (1982).
8. Pan, J., Leygraf, C., Jargelius-Pettersson, R. F. A. & Linden, J. Characterization of high-temperature oxide films on stainless steels by electrochemical-impedance spectroscopy. *Oxid. Met.* **50**, 431–455 (1998).
9. Cheng, X., Wang, Y., Dong, C. & Li, X. The beneficial galvanic effect of the constituent phases in 2205 duplex stainless steel on the passive films formed in a 3.5% NaCl solution. *Corros. Sci.* **134**, 122–130 (2018).
10. Frankel, G. S., Guillaumin, V. & Schmutz, P. Characterization of corrosion interfaces by the scanning Kelvin probe force microscopy technique. *J. Electrochem. Soc.* **148**, B163–B173 (2001).
11. Hurley, M. F. et al. Volta potentials measured by scanning Kelvin probe force microscopy as relevant to corrosion of magnesium alloys. *Corrosion* **71**, 160–170 (2015).
12. Örnek, C., Liu, M., Pan, J., Jin, Y. & Leygraf, C. Volta potential evolution of intermetallics in aluminum alloy microstructure under thin aqueous adlayers: a combined DFT and experimental study. *Top. Catal.* **61**, 1169–1182 (2018).
13. Örnek, C. et al. Characterization of 475 °C embrittlement of duplex stainless steel microstructure via canning Kelvin probe force microscopy and magnetic force microscopy. *J. Electrochem. Soc.* **164**, C207–C217 (2017).
14. Trasatti, S. in *Comprehensive Treatise of Electrochemistry: The Double Layer* (eds Bockris, J.O.M., Conway, B.E. & Yeager, E.) 45–81 (Springer US, Boston, MA, 1980).
15. Trasatti, S. The absolute electrode potential: an explanatory note. *Pure Appl. Chem.* **58**, 955–966 (1986).
16. Moore, W. J., Hummel, D. O., Trafara, G. & Holland-Moritz, K. *Physikalische Chemie* 1236 (Walter de Gruyter, New York, 1986).
17. Rüetschi, P. & Delahay, P. Potential at zero charge for reversible and ideal polarized electrodes. *J. Chem. Phys.* **23**, 697–699 (1955).
18. Jin, Y. et al. First-principle calculation of Volta potential of intermetallic particles in aluminum alloys and practical implications. *J. Electrochem. Soc.* **164**, C465–C473 (2017).
19. Bettini, E., Kivisäkk, U., Leygraf, C. & Pan, J. Study of corrosion behavior of a 2507 super duplex stainless steel: influence of quenched-in and isothermal nitrides. *Int. J. Electrochem. Sci.* **9**, 20 (2014).
20. Aoki, S., Ito, K., Yakuwa, H., Miyasaka, M. & Sakai, Ji Potential dependence of preferential dissolution behavior of a duplex stainless steel in simulated solution inside crevice. *Zair.-to-Kankyo* **60**, 363–367 (2011).
21. Lee, J.-S., Fushimi, K., Nakanishi, T., Hasegawa, Y. & Park, Y.-S. Corrosion behaviour of ferrite and austenite phases on super duplex stainless steel in a modified green-death solution. *Corros. Sci.* **89**, 111–117 (2014).
22. Maurice, V. et al. Effects of molybdenum on the composition and nanoscale morphology of passivated austenitic stainless steel surfaces. *Faraday Discuss.* **180**, 151–170 (2015).
23. Marcus, P. & Maurice, V. *Passivity of Metals and Alloys* (Materials Science and Technology, Wiley-VCH Verlag GmbH & Co. KgaA, 2006).
24. Laurent, B. et al. Dissolution and passivation of a silicon-rich austenitic stainless steel during active-passive cycles in sulfuric and nitric acid. *J. Electrochem. Soc.* **164**, C892–C900 (2017).
25. Örnek, C. et al. Hydrogen embrittlement of super duplex stainless steel—towards understanding the effects of microstructure and strain. *Int. J. Hydrog. Energy* **43**, 12543–12555 (2018).
26. Wilde, M., Beauport, I., Stuhl, F., Al-Shamery, K. & Freund, H. J. Adsorption of potassium on Cr_2O_3(0001) at ionic and metallic coverages and UV-laser-induced desorption. *Phys. Rev. B* **59**, 13401–13412 (1999).
27. W. Fredriksson. Depth profiling of the passive layer on stainless steel using photoelectron spectroscopy (2012).
28. Maurice, V., Marcus P. in *Progress in Corrosion Science and Engineering I: Progress in Corrosion Science and Engineering I* (eds Pyun, S.-I. & Lee, J.-W.) 1–58 (Springer New York, New York, NY, 2010).
29. Andresen, P.L. et al. in *Corrosion Mechanisms in Theory and Practice* (ed. Marcus, P.) 726 (Marcel Dekker, New York, 2002).
30. Natishan, P. M. & O'Grady, W. E. Chloride ion interactions with oxide-covered aluminum leading to pitting corrosion: a review. *J. Electrochem. Soc.* **161**, C421–C432 (2014).
31. Szklarska-Smialowska, Z. *Pitting Corrosion of Metals*. (National Association of Corrosion Engineers, Houstan, TX, USA, 1986).
32. Landolt, D., Mischler, S., Vogel, A. & Mathieu, H. J. Chloride ion effects on passive films on FeCr and FeCrMo studied by AES, XPS and SIMS. *Corros. Sci.* **31**, 431–440 (1990).
33. Grozovski, V., Vesztergom, S., Láng, G. G. & Broekmann, P. Electrochemical hydrogen evolution: H+ or H_2O reduction? A Rotating Disk Electrode Study. *J. Electrochem. Soc.* **164**, E3171–E3178 (2017).
34. Silverstein, R., Sobol, O., Boellinghaus, T., Unger, W. & Eliezer, D. Hydrogen behavior in SAF 2205 duplex stainless steel. *J. Alloy. Compd.* **695**, 2689–2695 (2017).
35. Mente, T. & Boellinghaus, T. Mesoscale modeling of hydrogen-assisted cracking in duplex stainless steels. *Weld. World* **58**, 205–216 (2014).
36. Olden, V., Thaulow, C. & Johnsen, R. Modelling of hydrogen diffusion and hydrogen induced cracking in supermartensitic and duplex stainless steels. *Mater. Des.* **29**, 1934–1948 (2008).
37. Gesnouin, C. et al. Effect of post-weld heat treatment on the microstructure and hydrogen permeation of 13CrNiMo steels. *Corros. Sci.* **46**, 1633–1647 (2004).
38. Guo, L. Q., Qin, S. X., Yang, B. J., Liang, D. & Qiao, L. J. Effect of hydrogen on semiconductive properties of passive film on ferrite and austenite phases in a duplex stainless steel. *Sci. Rep.* **7**, 3317 (2017).
39. Guo, L. et al. Effect of hydrogen on pitting susceptibility of 2507 duplex stainless steel. *Corros. Sci.* **70**, 140–144 (2013).
40. Li, M., Guo, L. Q., Qiao, L. J. & Bai, Y. The mechanism of hydrogen-induced pitting corrosion in duplex stainless steel studied by SKPFM. *Corros. Sci.* **60**, 76–81 (2012).
41. Lee, S. H. & Rasaiah, J. C. Proton transfer and the mobilities of the H+ and OH− ions from studies of a dissociating model for water. *J. Chem. Phys.* **135**, 124505-1–124505-10 (2011).
42. Mente, T. & Bollinghaus, T. Modeling of hydrogen distribution in a duplex stainless steel. *Weld. World* **56**, 66–78 (2012).
43. Wang, R., Li, J., Su, Y., Qiao, L. & Volinsky, A. A. Changes of work function in different deformation stage for 2205 duplex stainless steel by SKPFM, Procedia. *Mater. Sci.* **3**, 1736–1741 (2014).
44. Rohwerder, M. & Turcu, F. High-resolution Kelvin probe microscopy in corrosion science: scanning Kelvin probe force microscopy (SKPFM) versus classical scanning Kelvin probe (SKP). *Electrochim. Acta* **53**, 290–299 (2007).